

## STRUCTURAL INFORMATION ON THE ECR PLASMA BY X-RAY IMAGING

R. Rácz<sup>†</sup>, S. Biri, J. Pálinkás, Institute for Nuclear Research, Hungarian Academy of Sciences  
(Atomki), Debrecen, Hungary

D. Mascali, G. Castro, C. Caliri, L. Neri, F. P. Romano<sup>1</sup>, S. Gammino  
Istituto Nazionale di Fisica Nucleare – Laboratori Nazionali del Sud, Catania, Italy

<sup>1</sup>also at CNR-Istituto per i Beni Archeologici e Monumentali

### Abstract

Precise knowledge on the density distribution of the Electron Cyclotron Resonance Ion Source plasma is needed by several reasons: i) in order to possibly improve the quality parameters of the extracted ion beam (emittance, brightness) strongly linked to the plasma structure, ii) to correctly investigate the recently observed plasma instabilities and/or the implementation of alternative heating methods (e.g. modal conversion) iii) in order to improve the general microwave-to-plasma coupling efficiency, in view of a microwave-absorption oriented design of future ECRIS. The non-destructive spectroscopic diagnostic methods give information always corresponding to integration over the whole plasma volume. X-ray imaging by pin-hole camera can partly overcome this limitation. We performed volumetric and space resolved X-ray measurements at the ATOMKI ECRIS operated at lower frequencies than usual. The experimental setup in detail and the methods how the working parameters were selected will be shown. The integrated and photon-counting analyses of the collected plasma images show a strong effect of the frequency and magnetic field on the plasma structure and local energy content.

### INTRODUCTION

Imaging of the electron cyclotron resonance (ECR) plasmas by using CCD camera in combination with a pinhole is a non-destructive diagnostics method to record the strongly inhomogeneous spatial density distribution of the X-ray emitted by the plasma and by the chamber walls. This method can provide information on the location of the collisions between warm electrons and multiple charged ions/atoms, opening the possibility to investigate plasma structure in more details. Precise knowledge on the density distribution of the Electron Cyclotron Resonance Ion Source (ECRIS) plasma is needed by several reasons: 1) ECRISs provide worldwide highly charged ion beams for high energy accelerators and also the low energy ion beam of the source can be used in various fields of science (e.g. in atomic physics research, material science). In both application cases the parameters of the extracted ion beam are essentially and strongly determined by the shape, structure and quality of the ECR plasma. 2) Development path of the ECRISs is mainly

traced by the trend to apply stronger magnetic confinement with higher RF frequency. However the coupling efficiency may also improve by a microwave-absorption oriented design. The next generation of ECRISs may take into account the optimisation of the spatial density distribution of the plasma. 3) The correct investigation of the recently observed plasma instabilities [1] and/or the implementation of alternative heating methods (e.g. modal conversion [2]) are inconceivable with the few existing experimental data on the precise plasma density profiles.

In 2002 the Atomki ECR group carried out and published for the first time space-resolved plasma diagnostics measurements by a pinhole X-ray camera [3]. In 2014 a new series of volumetric and space resolved X-ray measurements have been carried out at the Atomki ECR ion source. The measurement was done in close collaboration between the Atomki ECRIS team (Debrecen, Hungary) and the ion source group of INFN-LNS (Catania, Italy). The aim was to study mainly the effect of the microwave frequency but also the effect of some setting parameters like microwave power and strength of the axial magnetic field on the plasma structure. The result of the volumetric measurements and the comparison of the two (2002 and 2014) experimental setups were published already in recent articles [4, 5].

Two different type of exposing methods were applied. In case of the spectrally integrated mode the photos are taken with several ten seconds exposure time. The only limitation for the exposure time was to avoid the blooming of the CCD (when a pixel in a CCD image sensor is overloaded). Individual pixels can be loaded by many X-ray photons, therefore the energy information of a given photon are lost. Photos were also taken in photon counting mode. In that case thousands of images are exposed with experimentally adjusted short (milliseconds) exposure time. Each pixel registered either 0 or 1 X-ray events. Therefore any individual pixel can be used as a single photon detector to spectrally resolve the plasma image. Because of the strong inhomogeneity of the plasma, region of interests (ROIs) were selected and the exposure time was settled by the intensity of the given region. The intensity of the other parts of the images was left out of consideration.

The huge amount of obtained experimental and then analysed data require the publication of the results in several papers. The present paper will show the methods how the working parameters for the pinhole camera measurements were selected. The presented preliminary

<sup>†</sup>rracz@atomki.hu

results will demonstrate the strong effect of the frequency and magnetic field on the spectrally integrated X-ray plasma images. Further detailed analysis of the integrated photos and the analysis of the more sophisticated photon counted images will be published elsewhere soon.

### EXPERIMENTAL SETUP

The experiment was performed at the Atomki ECR ion source [6]. The experimental setup presented in Figure 1. allows to take X-ray images and  $m/q$  spectra simultaneously, providing charge state distribution (CSD) and spectral, structural information on exactly the same plasma. Two detectors were applied at the injection side, alternatively. First the Silicon Drift Detector (SDD) (for volumetric measurements) was placed beyond a kapton foil ensuring vacuum break, and collimated by a lead cylinder with a drilled hole. Then the CCD X-ray camera (for spatially resolved measurements) made by 256x1024 pixels operational in the range of 500 eV – 10 keV was coupled to a lead pinhole (100  $\mu\text{m}$  in diameter) and placed along the axis, facing the chamber. The area of the circle shape injection plate was divided into two regions in the ratio 3:2. The smaller area was used for microwave and gas injection, while the larger part was closed by stainless steel mesh to keep a closed resonant cavity and to provide transparency for imaging. In addition, aluminum windows of variable thickness (range 1–6  $\mu\text{m}$ ) were used to screen the CCD from the visible and UV light emitted also by the plasma.

A High Purity Germanium (HPGe) detector was also placed on the axes, but at the other (extraction) side of the source beyond the 90-degree analysing magnet, after a quartz window. It was used for monitoring the X-rays emitted by the high energy electrons and it was collimated by lead blocks. The HPGe detected the radiation passing through the extraction hole of the plasma chamber.

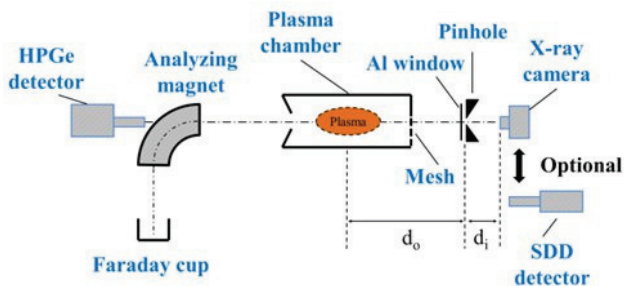


Figure 1: Schematic drawing of the X-ray diagnostic setup.

For microwave coupling low power (40 W) TWTA was used and the microwave frequency was varied between 12.8 and 13.4 GHz. The microwave signal was provided by HP 8350B sweep oscillator with HP 83590A plug-in (2 - 20 GHz). The injected power was measured at the closest possible point (at a distance of 130 cm from the plasma chamber entrance) by an RF probe after a directional coupler. The low power level (varied between 20 and 40 W) was decided in order to prevent high dead-times in the SDD detector and pixels-saturation in the

CCD camera. The ECR ion source was optimized for  $\text{Ar}^{4+}$  ions production. The gas pressure measured at the injection side of the ion source was  $P_{\text{inj}}=3.3 \cdot 10^{-6}$  mbar.

### SELECTION OF WORKING POINTS

During the measurements a wide range of external ion source setting parameters and technical solutions were tried and tested. Volumetric measurements (by SDD and by HPGe detectors) were done at different pumping microwave frequencies between 12.80-13.40 GHz, with 40 MHz steps (16 frequencies). Some of these frequencies proved to be better or worth than others, in terms of resulting higher or lower  $\text{Ar}^{4+}$  current.

In the preceding paper [4] several good agreements were found between the external beam features (analysed and total beam intensity, average charge, SDD counts) and the calculated plasma electron parameters (density, temperature, number of modes) vs microwave frequency. In Figure 2 the electron density, temperature and the extracted and analysed Ar beam current is drawn as a function of the frequency.

#### Frequency

For the integrated plasma images eight frequencies from 12.84 to 13.16 GHz with 80 MHz steps were selected while a limited number from them (so-called “representatives”) had to be selected for the time-consuming spectrally-resolved recordings. The 12.84 and 12.92 GHz frequencies were selected for this studies as being the two frequencies producing broad fluctuation in both X-ray flux and output current, while 13.24 GHz represents a significant frequency since the increase of output current does not correspond – as occurs for the other data – to a comparable increase of X-ray flux.

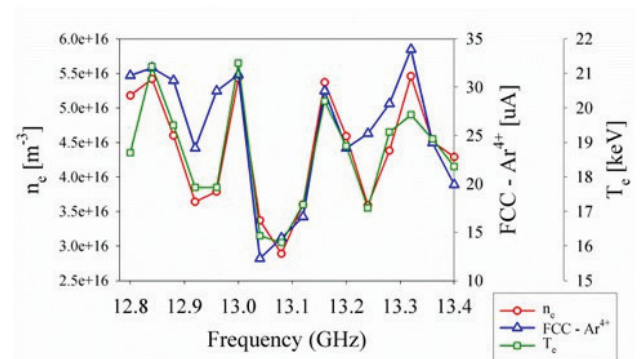


Figure 2: Trend of the electron density, temperature and  $\text{Ar}^{4+}$  current vs pumping frequency.

#### Magnification and the Thickness of the Al Window

The position of the pinhole respect to the plasma and to the CCD chip develops the magnification of the pinhole system. By varying the thickness of the Al-window the flux of the visible and UV part of the obtained spectra respect to the X-ray part can be justified. Both parameters were optimized.

Mounting  $D = 6$  micrometres Al-window (Figure 3 (a)) the window filtered strongly the X-ray radiation. In contrary,  $D = 1$  micrometres proved to be too thin (Figure 3 (b)), the picture is too noisy.  $D = 3$  micrometres (Figure 3 (c)) is a good compromise; this window was selected and used for the energy-resolved measurements.

The magnification ( $M$ ) is the quotient of  $d_i$  and  $d_o$  (image and object distances) as shown in Figure 1. Three average  $M$  values were set and tried: 0.082, 0.124 and 0.158. Also three different Al-windows were tested with thicknesses of 6, 1 and 3 micrometres ( $D$ ). These are altogether 9 combinations but among them only 3 were tested, as seen in Figure 3 (a) - (c). From the figures it is obvious that the largest magnification ( $M = 0.158$ ) can be and has to be applied, because it is still cover the important parts of the plasma. It is true however that the lowest middle plasma branch (as it is seen in the (d) pic-

ture) is not shown (outside) in the right picture. That is why for photon counting analysis this magnification and alignment were applied at the beginning (Fig. 3. (c)).

After that the pinhole camera was vertically tilted by a few degrees to “move back” that branch of the plasma into the picture. Then the camera was not moved anymore and the integrated images investigating the power dependence and the effect of the strength of the axial magnetic field were recorded using the alignment represented by Fig. 3 (d).

$M = 0.158$  magnification and  $D = 3$  micrometres thick aluminium window was used all the images cases presented in this paper. The only exception is the frequency dependence series because it was recorded at the earlier stage of the experiment. At that time the magnification and the window thickness were  $M = 0.082$  and  $D = 6$ , respectively.

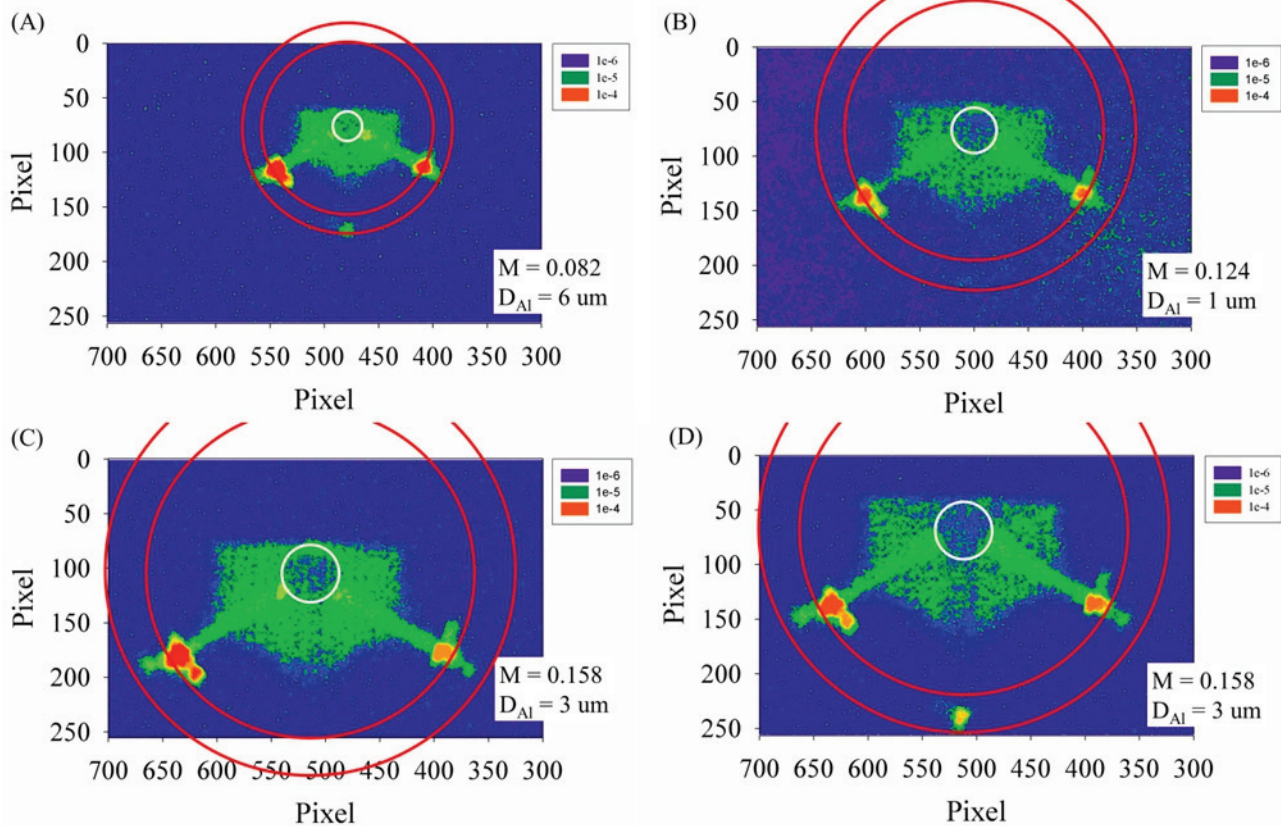


Figure 3: Integrated plasma images for the selection of the optimal magnification ( $M$ ) and Al-window thickness ( $D$ ). From (a) to (c) ( $M/D$ ): 0.082/6, 0.124/1, 0.158/3. For (d) only the alignment was changed respect to (c). All the images were normalised to 1 (total number of counts in each picture = 1) and mirrored by two axes to see exactly the original arrangement. The red circles roughly represent the contours of the farther (extraction side, small circle) and the closer (injection side, large circle) end-plates of the plasma chamber, respectively. The white circle shows the contour of the extraction hole.

## DEPENDENCE ON THE ECR SETTING PARAMETERS

The effect of some external setting parameters of the ion source (microwave frequency, axial magnetic field, microwave power) on the spectrally integrated images were recorded and studied. Due to the long exposure time (15 – 40 seconds) the spectral information in a given pixel is superposed and lost, however the changes in the shape, structure and local energy contents of the plasma is clearly visible in the images presented by this chapter.

### Frequency Dependence

The injected RF frequency was varied between 12.84 GHz and 13.16 GHz with 80 MHz steps. The microwave power coupled to the plasma chamber was 30 W. The strength of the magnetic trap was maximal (100 % coils currents). Because this wide set of frequencies were applied only at the first series of the measurement the magnification and the window thickness are  $M = 0.082$  and  $D = 6$ , respectively. The acquisition time was 15 seconds for each frame. Figure 4 shows the spectrally integrated plasma images taken at different frequencies.

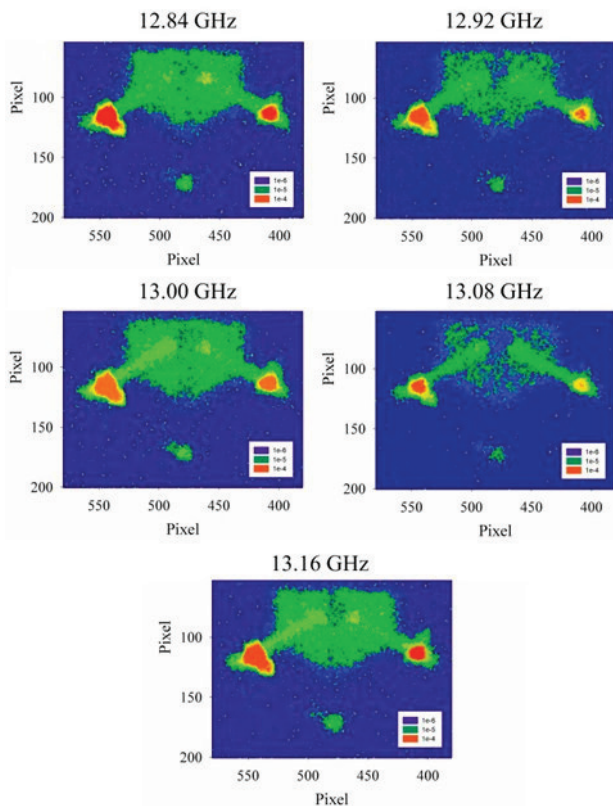


Figure 4: Spectrally integrated plasma images as function of the RF frequency. The images were normalised to 1 (total number of counts in each picture = 1) and mirrored by two axes to see exactly the original arrangement.

It is clear from the volumetric measurements that the intensity of X-ray photons emitted by the plasma strongly depends on the RF frequency and it is in strong correla-

tion with the mean charge state ( $\langle Q \rangle$ ) of the extracted ion beam [4]. Figure 4 clearly shows that the total counts obtained at the near axis regions (extraction hole) are also fluctuating. One can conclude that the emptier the near axis region the lower the  $\langle Q \rangle$ . This highlights the effect of the density distribution of the plasma to the ionization efficiency.

### Power Dependence

Effect of the microwave power to the integrated images was recorded. The frequency was fixed at 12.84 GHz. Spectrally integrated X-ray images were exposed when the microwave power coupled to the plasma chamber was 20 W, 30 W and 40W. The strength of the magnetic trap was maximal (100 % coils currents). The average magnification and the window thickness were  $M = 0.158$  and  $D = 3$ , respectively. The acquisition time was 40 seconds for each frame. The spectrally integrated plasma images as function of the injected microwave power can be seen in Figure 5. While the total count of the X-ray photos are increased with the microwave power the structure of the plasma was not changed remarkably.

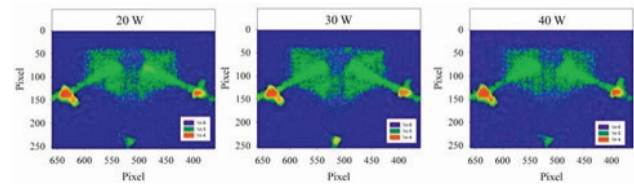


Figure 5: Spectrally integrated plasma images as function of the injected microwave power. The images were normalised to 1 and mirrored by two axes.

### Axial Magnetic Field Dependence

Effects of the decrease of the axial confinement on the integrated images were recorded. The frequency was fixed at 12.84 GHz. X-ray images were exposed when the axial magnetic field provided by the coils were decreased while the injected microwave power was fixed at 30 W. Images were taken when the coils current was set to 100%, 80% and 60% of the maximum output current of the power supply (Figure 6).

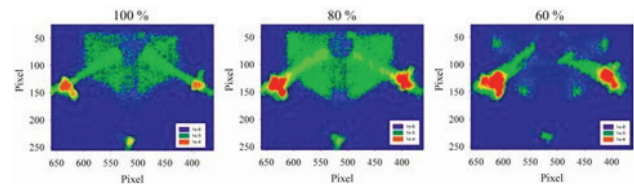


Figure 6: Spectrally integrated plasma images as function of the strength of the axial magnetic confinement. The average magnification and the window thickness are  $M = 0.158$  and  $D = 3$ , respectively. The acquisition time was 40 seconds for each frame. The images were normalised to 1 and mirrored by two axes.

Similarly to the effect of the microwave power the total counts of the images are increasing with the applied coils

current, meanwhile strong structural effect appear; the near axis region becomes emptier at each reduction step, the plasma is expanding and is shifting toward the plasma chamber wall. This shift can be explained by the radial expand of the resonant surface.

### SUMMARY

Experimental campaign with wide instrumentation was carried out to measure the volumetric and spatially resolved X-ray emission of the ECR plasma. Methods were shown how the working parameters for the pinhole camera measurements were selected. As preliminary results correlation between the global setting parameters of the plasma (axial magnetic field, RF frequency, microwave power) and the spatial distribution of the pinhole X-ray images were demonstrated: (1) strong effect of the RF frequency on the plasma images especially in the near axis region, (2) strong effect of the axial magnetic confinement on the radial dimensions of the plasma; the plasma is expanding and is shifting toward the plasma chamber wall meanwhile the plasma images in the near axis region becomes emptier at each reduction step, (3) no remarkably effect on the plasma structure as function of the externally coupled microwave power.

Further detailed analysis of the integrated photos and the analysis of the large amount and more sophisticated photon counted images are needed and will be published in a subsequent paper soon.

### ACKNOWLEDGEMENT

“This project has received funding from the European Union’s Horizon 2020 research and innovation program under grant agreement No 654002 (ENSAR2-MIDAS)”.

### REFERENCES

- [1] O. Tarvainen, T. Kalvas, H. Koivisto, J. Komppula, R. Kronholm, J. Laulainen, I. Izotov, D. Mansfeld and V. Skalyga, Kinetic instabilities in pulsed operation mode of a 14 GHz electron cyclotron resonance ion source, *Review of Scientific Instruments* 87 (2016) 02A701
- [2] G. Castro, D. Mascali, F. P. Romano, L. Celona, S. Gammino, D. Lanaia, R. Di Giugno, R. Miracoli, T. Serafino, F. Di Bartolo, N. Gambino and G. Ciavola, Comparison between off-resonance and electron Bernstein waves heating regime in a microwave discharge ion source, *Review of Scientific Instruments* 83 (2012) 02B501
- [3] S. Biri, A. Valek, T. Suta, E. Takács, Cs. Szabó, L. T. Hudson, B. Radics, J. Imrek, B. Juhász and J. Pálinkás, Imaging of ECR plasmas with a pinhole x-ray camera, *Review of Scientific Instruments* 75 (2004) 1420
- [4] D. Mascali, G. Castro, S. Biri, R. Rácz, J. Pálinkás, C. Caliri, L. Celona, L. Neri, F. P. Romano, G. Torrisi and Santo Gammino, Electron cyclotron resonance ion source plasma characterization by X-ray spec-

troscopy and X-ray imaging, *Review of Scientific Instruments* 87 (2016) 02A510

- [5] R. Rácz, S. Biri, J. Pálinkás, D. Mascali, G. Castro, C. Caliri, F. P. Romano and S. Gammino, X-ray pinhole camera setups used in the Atomki ECR Laboratory for plasma diagnostics, *Review of Scientific Instruments* 87 (2016) 02A741
- [6] S. Biri, R. Rácz and J. Pálinkás, Status and special features of the Atomki ECR ion source, *Review of Scientific Instruments* 83 (2012) 02A341